Phase-matched emission of few high-harmonic orders from a helium gas cell

Sven Teichmann,[a] Peter Hannaford, and Lap Van Dao
ARC Centre of Excellence for Coherent X-Ray Science, Centre for Atom Optics and Ultrafast Spectroscopy, Swinburne University of Technology, Melbourne 3122, Australia

(Received 15 March 2009; accepted 11 April 2009; published online 29 April 2009)

We report on femtosecond-laser-based generation of a few phase-matched high-order harmonics in a helium semi-infinite gas cell. The harmonic beam consists of effectively four to six intense orders with wavelengths around 9.5 nm. By varying the effective interaction length, we observe the effects of coherence length related to plasma formation and the Gouy phase shift on the output. The atomic scattering factors for photoabsorption, the effective propagation lengths ($l_{\mathrm{eff,He}} \approx 1$ mm, $l_{\mathrm{eff,Ar}} \approx 7.2$ mm), and the energy conversion efficiencies ($\varepsilon_{\mathrm{He}} \approx 10^{-7}$, $\varepsilon_{\mathrm{Ar}} \approx 5 \times 10^{-7}$) are deduced for harmonic generation in helium (77th to 95th orders) and also argon (21st to 27th orders) for comparison. © *2009 American Institute of Physics*. [DOI: 10.1063/1.3127521]

Femtosecond-laser-driven high-harmonic generation (HHG) sources provide spatially and temporally coherent ultrashort pulses of extreme-ultraviolet radiation and soft x rays.[1] By their nature, these small-scale and highly versatile sources produce a laserlike beam that consists of multiple longitudinal coherent modes. The harmonic emission can be tailored according to the experimental requirements for applications in atomic and molecular spectroscopy, condensed matter physics, imaging on the (sub-)nanoscale, and plasma physics.[2–6] Control over the characteristics of the output, which include the brightness or flux, the spatial and temporal coherence properties, and the spectral range of the harmonic orders, is crucial and depends strongly on the interaction geometry.

In principle, the characteristics of the laser beam are imprinted onto the harmonic beam. Nevertheless, the chosen interaction geometry and the intrinsic process of plasma formation lead to a complex spatially and temporally dependent induced nonlinear polarization in the medium and strongly determine the conversion efficiency, the spatial, spectral, and temporal properties, and the coherence of the harmonic emission. Due to its coherent nature, HHG emission is increasingly being used for coherent diffractive imaging (CDI).[7,8] We have recently performed multiple-wavelength CDI (Ref. 8) by using several phase-matched harmonics from an argon gas cell in the wavelength range ~25–40 nm. For this application the generation of just a few harmonic orders with high flux is essential.[9,10]

In our previous work,[9,10] we focused on the phase-matched emission of just a few harmonic orders around ~30 nm in an argon gas cell where the absorption coefficient varies significantly with wavelength. We showed that the HHG by a freely propagating fundamental laser beam in a gas cell has the same benefits of homogeneous phase matching as in hollow-core fibers at low gas pressures.[11] Because a much higher gas pressure can be applied in a gas cell, the optimal interaction length needs to be studied in more detail in order to balance the harmonic generation process with the reabsorption. In a helium gas cell, high-order harmonics with much shorter wavelengths can be achieved and the optimal gas pressure is typically very high. Under these conditions, the harmonic emission has a significantly shorter coherence length and the variation of the absorption coefficient is very different to that in an argon gas cell.

In this paper, we report on the generation of the 77th (H77) to 95th (H95) harmonic orders in a helium semi-infinite gas cell with energy conversion efficiency one-fifth of that achieved in an argon gas cell, but with much shorter wavelength. The coherence lengths which are related to plasma formation and Gouy phase shift, the relative position of the laser foci in the gas cell and the effective interaction lengths between the fundamental laser and the harmonic field, and the generated photon flux are determined and discussed. Effectively, the harmonic beam is confined to four to six intense harmonic orders around ~9.5 nm. Thus, this source is a potential source for time-resolved spectroscopy, such as femtosecond photoelectron spectroscopy, in the extreme ultraviolet and soft x-ray region,[5] and for multiple-wavelength CDI with high spatial resolution,[8] where few harmonic orders of short wavelength or a dominant photon energy are required and any optics in the harmonic beam path, such as reflection gratings, are undesirable.

A 1 kHz multipass chirped-pulse amplifier system produces 30 fs pulses centered at $\lambda_0 = 805$ nm. The unapertured and unfocused laser beam has a $(1/e^2)$ diameter of 12 mm and an energy of 1.9 mJ per pulse. A calibrated aperture is applied to the beam before it is focused into a 260-mm-long helium (argon) gas cell of pressure 810 Torr (58 Torr) by a lens of focal length 400 nm. The *in vacuo* $(1/e^2)$ radius of the focused intensity distribution of the laser beam, when truncated to a diameter of 8.25 mm (6.25 mm) for helium (argon), is $w_{0,\mathrm{He}} \approx 34$ μm ($w_{0,\mathrm{Ar}} \approx 43$ μm),[12] and the Rayleigh range is $z_{0,\mathrm{He}} \approx 4.4$ mm ($z_{0,\mathrm{Ar}} \approx 7.2$ mm). The pressure, aperture diameter, energy of the laser pulses, position of the laser focus relative to the exit of the gas cell, and chirping of the laser pulses are optimized in an iterative procedure for maximum flux of all available harmonics. For the helium (argon) gas cell a silver or zirconium (aluminum) metal filter is applied to separate the harmonics from the fundamental laser beam. A 26.8×26.8 mm^2 charge-coupled device (CCD) chip of pixel size 20×20 μm^2 (Princeton Instru-

[a]Author to whom correspondence should be addressed. Electronic mail: steichmann@swin.edu.au.

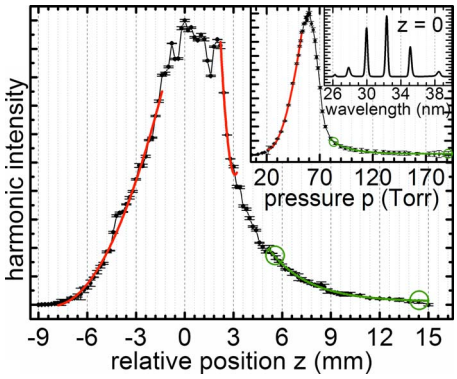

FIG. 1. (Color online) Argon gas cell: harmonic intensity vs laser focus position. Inset: harmonic intensity vs pressure, and spectral power distribution for position of maximum flux. Red solid line: quadratic fit for phase-matched harmonic emission. Green dashed line (marked by large circles): fit of exponential decay curve.

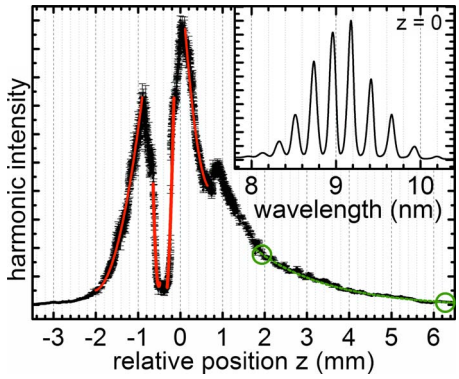

FIG. 2. (Color online) Helium gas cell: harmonic intensity vs laser focus position. Inset: spectrum for position of maximum flux. Red solid line: quadratic fit for phase-matched harmonic emission. Green dashed line (marked by large circles): fit of exponential decay curve.

ments PI-SCX 1340×1340 pixels) is used as a detector and is positioned 0.94 m from the exit of the gas cell. Optionally, a grazing incidence spectrometer (GIMS #4—Setpoint) can be inserted into the beam path. The spectrally resolved far-field beam profile can then be detected along the height of the exit slit of the spectrometer. Alternatively, *in situ* spectral analysis can be performed by applying the maximum entropy method to the interference pattern of a Young double slit pair illuminated with the emission of the harmonic source.[13]

The intensity of the qth harmonic order in nonabsorbing gas scales as $I_q \propto N_a^2 \sin c^2(\Delta k l_{\mathrm{eff}})$,[11,14] where $\sin c(x) = \sin(x)/x$, N_a is the atom density, l_{eff} is the effective interaction length between the fundamental laser field and the nonlinear medium, and Δk is the phase mismatch between the fundamental and the harmonic field. If the atomic response is constant or varies only slightly over a propagation length that corresponds to the coherence length and the phases between the fundamental and harmonic field are matched, then the harmonic intensity scales as $I_q \propto N_a^2$ or $I_q \propto p^2$, where p is the pressure of the generating gaseous medium. Also, the harmonic intensity will scale as $I_q \propto \Delta z^2$ with increasing interaction length Δz.

The inset of Fig. 1 shows the intensity dependence on the pressure in the argon gas cell. The optimized value for the pressure is $p_{\mathrm{Ar}}=58$ Torr. For 20 Torr $< p_{\mathrm{Ar}} <$ 55 Torr harmonic emission is phase-matched and $I_q \propto N_{a,\mathrm{Ar}}^2 \propto p_{\mathrm{Ar}}^2$ (fitted solid red line). For $p_{\mathrm{Ar}} \gg 58$ Torr, reabsorption by the gas dominates, and an exponential decay curve can be fitted (dashed green line, marked by large circles). An effective interaction length between the fundamental laser field and the nonlinear medium of $l_{\mathrm{eff,Ar}} \approx 7.2$ mm can be extracted from the exponential decay constant $C_{\mathrm{Ar},p} = 2 l_{\mathrm{eff,Ar}} r_o \langle\lambda\rangle_{\mathrm{Ar}} \langle f_2\rangle_{\mathrm{Ar}} / (k_B T) \approx 0.059(4)$,[15] where r_o is the classical electron radius, $\langle\lambda\rangle_{\mathrm{Ar}} \approx 30$ nm is the average wavelength of the spectral power distribution (see inset for $p = 100$ Torr), k_B is the Boltzmann constant, and T is the temperature. The (imaginary part of the) atomic scattering factor for photoabsorption $\langle f_2\rangle_{\mathrm{Ar}}$ is extracted from the measurement of the dependence of intensity on the position of the laser focus in Fig. 1. The x-axis is calibrated such that the global intensity maximum is at $z=0$ mm. The laser focus is close to the exit plane and deeper inside the gas cell for larger values of z. The harmonic intensity scales quadratically with increasing values of z over a propagation length of ≈ 7 mm (fitted solid red line) and thus indicates phase-matched harmonic emission. This value agrees very well with the value $l_{\mathrm{eff,Ar}} \approx 7.2$ mm extracted from the exponential decay constant $C_{\mathrm{Ar},p}$ and is also comparable to $z_{0,\mathrm{Ar}} \approx 7.2$ mm. Thus, when the laser focus is properly positioned inside the gas cell, the HHG is phase-matched over the whole Rayleigh range of the laser focus. When the laser focus is placed deeper inside the gas cell, reabsorption by the generating medium dominates and an exponential decay curve can be fitted (dashed green line, marked by large circles). An average value of the (imaginary part of the) atomic scattering factor for photoabsorption $\langle f_2\rangle_{\mathrm{Ar}} \approx 1.4$ can be extracted from the decay constant. This value for $\langle f_2\rangle_{\mathrm{Ar}}$ compares reasonably well with the average literature value $\Sigma f_q w_q / \Sigma w_q \approx 1.1$,[15] where f_q is the atomic scattering factor of the qth harmonic order with center wavelength λ_q of spectral weight w_q (inset $z=0$ mm of Fig. 1). For $z=0$ mm we calculate a total of $\sim 5\times10^{10}$ generated harmonic photons per second or an energy conversion efficiency of $\varepsilon_{\mathrm{Ar}} \approx 5\times10^{-7}$.

Comparison of the dependence of the HHG intensity on the position of the laser focus in the argon gas cell with the helium gas cell can be made by means of Fig. 2 with the same experimental procedure. The x-axis calibration is consistent with Fig. 1, but comparing the settings of the translation stage for the focusing lens reveals that the laser focus is $\Delta \approx 2.6$ mm deeper inside the gas cell. When varying the position of the laser focus, a coherence length-induced oscillating intensity can be observed with the global and local maximum separated by $\Delta z_{\mathrm{He}} \approx 900$ μm. This value is consistent with the propagation length over which phase matching can be observed and the intensity scales quadratically with z (fitted solid red line). The Gouy phase-related coherence length is given by $l_{c,\mathrm{Gouy}}(z) = \pi(z_0 + z^2/z_0)/q$. At the focus $l_{c,\mathrm{Gouy}}(0) = \pi z_{0,\mathrm{He}}/q$ ranges from ≈ 141 to 178 μm for H97 to H77. However, when taking into account that the effective propagation length in argon is $l_{\mathrm{eff,Ar}} \approx 7.2$ mm and that the laser focus is $\Delta \approx 2.6$ mm deeper inside the gas cell when filled with helium, $l_{c,\mathrm{Gouy}}(z = l_{\mathrm{eff,Ar}} + \Delta \approx 1\ \mathrm{cm}) \approx 1$ mm when evaluated at that distance from the laser focus, which is comparable with Δz_{He}. Calculating the minimum intensity to generate the qth harmonic order according to the semiclassical cutoff and employing the Ammosov–Delone–Krainov model[16] to determine the level of ionization η_q of helium at the end of the laser pulse allows the value of the plasma-related coherence length $l_{c,\mathrm{plasma}}$

$=4\pi^2 m_e/(q\lambda_0 e^2 \mu_0 \eta_q p)$ to be established and to be compared with $l_{c,\mathrm{Gouy}}(z \approx 1\ \mathrm{cm})$, where m_e and e are the electron mass and charge, λ_0 is the center wavelength of the fundamental laser field, and μ_0 is the magnetic constant. For H77 to H97, $l_{c,\mathrm{plasma}}$ ranges from ~538 to 66 μm and is significantly shorter than Δz_{He}. Thus, when the laser focus is properly positioned inside the gas cell, we can exploit the Gouy phase shift to phase-match the harmonics H77 to H97 over a propagation length of $l_{\mathrm{eff,He}} \approx 1$ mm. When the laser focus is placed deeper inside the gas cell, harmonic emission is dominated by reabsorption by the generating gas and an exponential decay curve can be fitted (dashed green line, marked by large circles). An average value of the (imaginary part of the) atomic scattering factor for photoabsorption $\langle f_2 \rangle_{\mathrm{He}} \approx 0.39$ can be extracted from the decay constant $C_{\mathrm{He},z}=2p_{\mathrm{He}} r_o \langle \lambda \rangle_{\mathrm{He}} \langle f_2 \rangle_{\mathrm{He}}/(k_B T) \approx 0.556(8)$,[15] where $p_{\mathrm{He}} = 810$ Torr and $\langle \lambda \rangle_{\mathrm{He}} \approx 9.5$ nm is the average wavelength of the spectral power distribution of the harmonics H77 to H95 (inset of Fig. 2). This value for $\langle f_2 \rangle_{\mathrm{He}}$ compares very well with the average literature value $\Sigma f_q w_q / \Sigma w_q \approx 0.38$.[15] The exponential decay exhibits modulations of order ≤ 538 μm, which we attribute to intrinsic plasma formation. For $z = 0$ mm, we calculate a total of $\sim 5 \times 10^9$ generated harmonic photons per second, or an energy conversion efficiency of $\varepsilon_{\mathrm{He}} \approx 10^{-7}$, which is to be compared with $\varepsilon_{\mathrm{Ar}} \approx 5 \times 10^{-7}$ for the argon gas cell.

In conclusion, we have been able to control the generation of just a few coherent modes H77 to H95 in a helium semi-infinite gas cell with an energy conversion efficiency of one-fifth of that achieved in an argon semi-infinite gas cell. Macroscopic phase matching by exploiting the Gouy phase shift is achieved when the laser focus is properly placed inside the gas cell and deeper than in the case of the argon gas cell. Given the reasonably efficient generation of effectively four to six intense harmonic orders around ~9.5 nm, we propose to employ this helium-based HHG source for multiple-wavelength CDI.[8] So far, we have achieved image reconstruction of a nonperiodic object with a resolution of <100 nm using multiple-harmonic orders of the argon gas cell. As $\langle \lambda \rangle_{\mathrm{He}} \approx 9.5$ nm and $\langle \lambda \rangle_{\mathrm{Ar}} \approx 30$ nm, we expect a significantly higher resolution of the reconstruction.

[1] A. Rundquist, C. G. Durfee III, Z. Chang, C. Herne, S. Backus, M. M. Murnane, and H. C. Kapteyn, Science **280**, 1412 (1998).
[2] S. Marchesini, H. N. Chapman, S. P. Hau-Riege, R. A. London, A. Szoke, H. He, M. R. Howells, H. Padmore, R. Rosen, J. C. H. Spence, and U. Weierstall, Opt. Express **11**, 2344 (2003).
[3] E. A. Gibson, A. Paul, N. Wagner, R. Tobey, D. Gaudiosi, S. Backus, I. P. Christov, A. Aquila, E. M. Gullikson, D. T. Attwood, M. M. Murnane, and H. C. Kapteyn, Science **302**, 95 (2003).
[4] H. C. Kapteyn, M. M. Murnane, and I. P. Christov, Phys. Today **58** (3), 39 (2005).
[5] M. Bauer, J. Phys. D **38**, R253 (2005).
[6] C. Figueira de Morisson Faria, P. Salières, P. Villain, and M. Lewenstein, Phys. Rev. A **74**, 053416 (2006).
[7] R. L. Sandberg, C. Song, P. W. Wachulak, D. A. Raymondson, A. Paul, B. Amirbekian, E. Lee, A. E. Sakdinawat, C. La-O-Vorakiat, M. C. Marconi, C. S. Menoni, M. M. Murnane, J. J. Rocca, H. C. Kapteyn, and J. Miao, Proc. Natl. Acad. Sci. U.S.A. **105**, 24 (2008).
[8] B. Chen, R. A. Dilanian, S. Teichmann, B. Abbey, A. G. Peele, G. J. Williams, P. Hannaford, L. Van Dao, H. M. Quiney, and K. A. Nugent, Phys. Rev. A **79**, 023809 (2009).
[9] L. Van Dao, S. Teichmann, J. Davis, and P. Hannaford, J. Appl. Phys. **104**, 023105 (2008).
[10] L. Van Dao, S. Teichmann, and P. Hannaford, Phys. Lett. A **372**, 5254 (2008).
[11] C. G. Durfee III, A. R. Rundquist, S. Backus, C. Herne, M. M. Murnane, and H. C. Kapteyn, Phys. Rev. Lett. **83**, 2187 (1999).
[12] Z. L. Horváth and Z. Bor, Opt. Commun. **222**, 51 (2003).
[13] R. A. Dilanian, B. Chen, H. M. Quiney, K. A. Nugent, S. Teichmann, and L.V. Dao, Opt. Lett. **33**, 2341 (2008).
[14] E. Constant, D. Garzella, P. Breger, E. Mével, Ch. Dorrer, C. Le Blanc, F. Salin, and P. Agostini, Phys. Rev. Lett. **82**, 1668 (1999).
[15] Center for X-Ray Optics, Lawrence Berkeley National Laboratory (USA), http://www.cxro.lbl.gov, X-Ray Interactions with Matter, http://henke.lbl.gov/optical_constants.
[16] M. V. Ammosov, N. B. Delone, and V. P. Krainov, Sov. Phys. JETP **64**, 1191 (1986).